RL-TR-95-266
Final Technical Report
February 1996

FUNDAMENTAL CHARACTERIZATION OF ADVANCED ORGANIC POLYMERS FOR OPTICAL WAVEGUIDE DEVICES

Washington University

Robert R. Krchnavek and Daniel L. Rode (Washington University)
and Raymond K. Boncek (Rome Laboratory)

APPROVED FOR PUBLIC RELEASE; DISTRIBUTION UNLIMITED.

Rome Laboratory
Air Force Materiel Command
Rome, New York

DISCLAIMER NOTICE

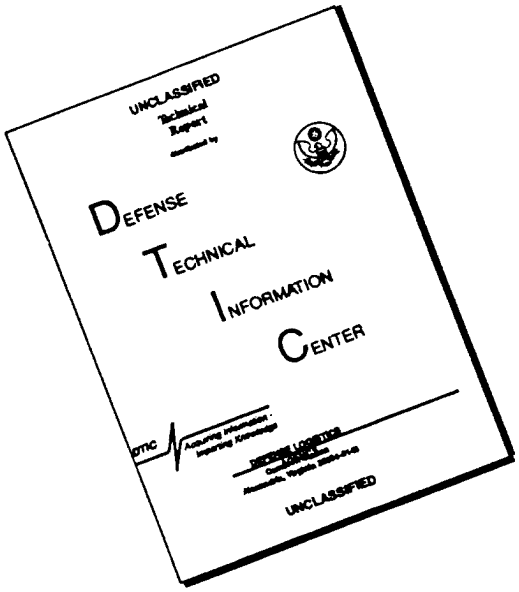

THIS DOCUMENT IS BEST QUALITY AVAILABLE. THE COPY FURNISHED TO DTIC CONTAINED A SIGNIFICANT NUMBER OF PAGES WHICH DO NOT REPRODUCE LEGIBLY.

This report has been reviewed by the Rome Laboratory Public Affairs Office (PA) and is releasable to the National Technical Information Service (NTIS). At NTIS, it will be releasable to the general public, including foreign nations.

RL-TR-95-266 has been reviewed and is approved for publication.

APPROVED: 

RAYMOND K. BONCEK
Project Engineer

FOR THE COMMANDER: 

GARY D. BARMORE, Major, USAF
Deputy Director of Surveillance & Photonics

If your address has changed or if you wish to be removed from the Rome Laboratory mailing list, or if the addressee is no longer employed by your organization, please notify Rome Laboratory/ (OCPA), Rome NY 13441. This will assist us in maintaining a current mailing list.

Do not return copies of this report unless contractual obligations or notices on a specific document require that it be returned.

REPORT DOCUMENTATION PAGE

Form Approved
OMB No. 0704-0188

1. AGENCY USE ONLY (Leave Blank)	2. REPORT DATE	3. REPORT TYPE AND DATES COVERED
	February 1996	Final Feb 94 - Feb 95

4. TITLE AND SUBTITLE

FUNDAMENTAL CHARACTERIZATION OF ADVANCED ORGANIC POLYMERS FOR OPTICAL WAVELENGTH DEVICES

5. FUNDING NUMBERS

C - F30602-94-C-0006
PE - 62702F
PR - 4600
TA - P1
WU - PW

6. AUTHOR(S)

Robert R. Krchnavek and Daniel L. Rode (Washington Univ.)
and Raymond K. Boncek (Rome Laboratory)

7. PERFORMING ORGANIZATION NAME(S) AND ADDRESS(ES)

Washington University
Campus Box 1054
One Brookings Drive
St. Louis MO 63130-4899

8. PERFORMING ORGANIZATION REPORT NUMBER

N/A

9. SPONSORING/MONITORING AGENCY NAME(S) AND ADDRESS(ES)

Rome Laboratory/OCPA
25 Electronic Pky
Rome NY 13441-4515

10. SPONSORING/MONITORING AGENCY REPORT NUMBER

RL-TR-95-266

11. SUPPLEMENTARY NOTES

Rome Laboratory Project Engineer: Raymond K. Boncek/OCPA/(315) 330-2937

12a. DISTRIBUTION/AVAILABILITY STATEMENT

Approved for public release; distribution unlimited.

12b. DISTRIBUTION CODE

13. ABSTRACT (Maximum 200 words)

Organic polymers doped with non-centrosymmetric chromophores have been suggested as viable candidates for organic based, active, electrooptic devices. While some investigators have shown working devices using several chromophores, the vast majority of work in this area is concentrating on measuring the electrooptic effect in the chromophore, and not the net result after the device has been fabricated. In this report, we document our efforts at characterizing guest/host electrooptic systems processed into structures representative of typical optical switch/modulator structures.

14. SUBJECT TERMS

Polymer, Organic, Chromophore, Waveguide, Optic, Electrooptic, Switch, Modulator, Pockels coefficient, DR-1, DR-13

15. NUMBER OF PAGES

20

16. PRICE CODE

17. SECURITY CLASSIFICATION OF REPORT	18. SECURITY CLASSIFICATION OF THIS PAGE	19. SECURITY CLASSIFICATION OF ABSTRACT	20. LIMITATION OF ABSTRACT
UNCLASSIFIED	UNCLASSIFIED	UNCLASSIFIED	UL

NSN 7540-01-280-5500

Standard Form 298 (Rev 2-89)
Prescribed by ANSI Std. Z39-18
298-102

TABLE OF CONTENTS

1 Introduction

Organic polymers doped with non-centrosymmetric chromophores have been suggested as viable candidates for organic based, active, electrooptic devices [1]. While some investigators have shown working devices using several chromophores, the vast majority of work in this area is concentrating on measuring the electrooptic effect in the chromophore, and not the net result after the device has been fabricated. In this final report, we document our efforts at characterizing guest/host electrooptic systems processed into structures representative of typical optical switch/modulator structures.

2 The Electrooptic Effect

As a brief review, we begin by describing the electrooptic effect. We restrict our attention to crystalline materials in this section and advance the topic to organic polymers in the next section. It is instructive to consider the electrooptic effect at both the macroscopic level as well as the molecular level. The electrooptic effect arises due to the fundamental electronic properties at the molecular level. Because the effect originates at the molecular level, one must consider this when fabricating organic polymers to maximize the electrooptic effect. On the other hand, the electrooptic effect as viewed from a macroscopic viewpoint is responsible for numerous switching/modulating devices. Finally, figures of merit for various materials come from understanding both the fundamental properties of the electrooptic effect (molecular level) as well as the specific switching/modulating applications (macroscopic level).

We begin at the macroscopic level by considering elementary electromagnetics and temporarily ignoring the vector nature of the fields. The electric flux density in a *linear* and *isotropic* material is given by

$$D = \varepsilon_0 E + P = \varepsilon_0(1 + \chi_e)E = \varepsilon_0 \varepsilon_r E \tag{1}$$

where D is the electric flux density in C/m^2, ε_0 is the permittivity of free space (8.854×10^{-12} F/m), E is the electric field in V/m, P is the polarization, χ_e is the electric susceptibility, and ε_r is the relative permittivity. From (1), we can see that the polarization is given by

$$P = \varepsilon_0 \chi_e E \, . \tag{2}$$

In a linear material, the electric susceptibility is independent of E. However, in a nonlinear material, the susceptibility is a function of E and the polarization is then given by

$$P = P_0 + \chi^{(1)}E + \chi^{(2)}EE + \chi^{(3)}EEE + \ldots \tag{3}$$

where P_0 is the static polarization, and $\chi^{(1)}$, $\chi^{(2)}$, and $\chi^{(3)}$ are the linear, second-order, and third-order nonlinearity terms, respectively.

In electrooptic work, we are less interested in the polarization than in how the electric field modifies the refractive index. The refractive index is defined as

$$n = \sqrt{\varepsilon_r} \tag{4}$$

where we are assuming low-loss dielectrics. Using equations (1) and (4), the refractive index can be defined in terms of the polarization

$$n = \sqrt{1 + P / \varepsilon_0 E} \,. \tag{5}$$

In a linear material, the refractive index is independent of the electric field. However, in a nonlinear material, substituting the polarization (3) into (5) yields

$$n = \sqrt{1 + \frac{P_0}{\varepsilon_0 E} + \frac{\chi^{(1)}}{\varepsilon_0} + \frac{\chi^{(2)}}{\varepsilon_0} E + \frac{\chi^{(3)}}{\varepsilon_0} EE + \ldots} \tag{6}$$

which indicates that the refractive index is a function of the electric field.

In general, the refractive index is not a strong function of E. Therefore, it is customary to expand the refractive index in a Taylor's series

$$n(E) = n + a_1 E + \tfrac{1}{2} a_2 E^2 + \ldots \tag{7}$$

where n is assumed to indicate the refractive index with no applied field, i.e., $n(0)$. The coefficients of the Taylor series expansion (a_1, a_2, ...) can be rewritten in the following form

$$n(E) = n - \tfrac{1}{2} r n^3 E - \tfrac{1}{2} s n^3 E^2 + \ldots \tag{8}$$

where r is the linear electrooptic coefficient (Pockels coefficient) and s is the quadratic electrooptic coefficient (Kerr coefficient). These unusual coefficients for the Taylor series expansion result from considering the electric impermeability. The electric impermeability is defined as

$$\eta = \varepsilon_0 / \varepsilon = 1 / n^2 \,. \tag{9}$$

A small change in the electric permeability can be described by

$$\Delta\eta = \Delta\left(\frac{1}{n^2}\right) = rE + gE^2 = \frac{d\eta}{dn}\Delta n \tag{10}$$

where r and g are terms in a Taylor series expansion for the impermeability. Since $\Delta n = a_1 E + 1/2 a_2 E^2$ and $d\eta/dn = -2/n^3$, the coefficients for the Taylor series expansion of the refractive index (a_1, a_2, ...) can be rewritten in terms of r and g. The linear electrooptic coefficient, r, is the primary quantity used to evaluate the electrooptic effect in materials used for active devices such as switches and modulators.

3 The Electrooptic Effect in Organic Polymers

The electrooptic effect described above can also be present in specially formulated organic polymers. Usually, this involves incorporating a specific molecule that exhibits a strong molecular electrooptic effect into an organic polymer matrix. This molecule, usually designated as a chromophore, must be a non-centrosymmetric molecule in order to exhibit an electrooptic effect. There are several available chromophores and this has been an intense area of research in recent years.

There are three primary methods of incorporating the chromophore into the polymer matrix. The first is the guest/host system. In this system, a guest chromophore is simply mixed into the host polymer matrix. This technique is quite simple but is known to be one of the least stable systems. However, it is ideal for evaluating various chromophore/matrix combinations in actual device structures. The second method is to incorporate the chromophore as a side-chain in the host matrix. This requires organic chemistry synthesis to substitute the chromophore for a radical on the polymer matrix. While more stable than the guest/host system, the synthesis chemistry can be quite difficult. Finally, incorporating the chromophore into the backbone of the polymer matrix is the most stable but also requires the greatest amount of chemical synthesis. We have used the guest/host system in this work but are continuing to explore alternatives.

In addition to incorporating the chromophore into the polymer matrix, the chromophores need to be aligned so that their individual electrooptic effects are additive. This is a fundamental difference between the electrooptic effect in organic polymers versus crystalline structures. In crystals, the regular alignment of atoms assures that the unit cell electrooptic effect is additive throughout the crystal. However, in a non-crystalline organic polymer, the chromophores need to be aligned to form a pseudo-crystal structure. Although there are various methods of aligning the individual chromophores, the most widely used method consists of applying a strong electric field (100 V/μm) while raising the organic film above its glass transition temperature. The film is then slowly cooled while maintaining the electric field to assure some degree of alignment. This process is known as poling.

From the above discussion, we can see that the requirements of fabricating an organic film with a strong electrooptic effect are threefold: (*i*) the chosen chromophore must have a strong electrooptic effect; (*ii*) one must be able to incorporate a significant amount of the chromophore into the polymer matrix; (*iii*) the film must be efficiently poled and remain that way at room temperature.

We have explored two similar chromophores in two polymer matrices. The chromophores are: disperse red-1 (DR-1) and disperse red-13 (DR-13). The polymer matrices are poly-methylmethacrylate and a mixture of photopolymerizable di/tri acrylates.

4 Materials Characterization

Essential to the development of organic polymers for electrooptic device applications is a strong effort in the fundamental characterization of organic polymers and electrooptic molecules. Our work in this area is based upon the guest/host system for electrooptic effects in organic polymers. The characterization should consist of evaluating the host material with and without guest molecules present. Previously, we have reported on several aspects of a viable host material – photopolymerizable di/tri acrylates [2]. These materials have been characterized in terms of their optical losses at 780, 1000, and 1300 nm in single-mode and multimode optical waveguides. Their mechanical properties and degree of crosslinking have been evaluated using differential scanning calorimetry and dynamic mechanical analysis. Finally, we have demonstrated that the refractive index can be controlled by proper mixing of high- and low-index resins.

The addition of an electrooptic chromophore to a host polymer matrix will likely modify both the refractive index and the optical loss. If the addition of the chromophore lowers the refractive index of the host material below that of the cladding layer, the waveguide structure will no longer guide. Also, if the addition of the chromophore dramatically increases the waveguide loss, optical signal throughput will suffer. We have evaluated the change in refractive index of the host material after inclusion of the guest chromophore. The change in the refractive index is relatively small and can be engineered around by the proper mixture of low-index and high-index polymer resins. Our initial experiments in measuring the absorption effects indicate that the chromophore increases the absorption coefficient but not to such an extent that practical devices cannot be realized.

For measuring the electrooptic coefficient in the guest/host films, we are currently using a transverse modulation technique. A description of the technique follows.

Begin by consider a drawing of the physical setup (See Figure 1.) Assume for the moment that the light from the laser diode is perfectly coherent and monochromatic, and of single polarization. Also assume that by the time this light passes through the fiber and reaches the first polaroid that the angle of polarization of the light has some component along the line of polarization of the polarizer. The light emitted from the polarizer and imaged onto the input to the waveguide can then be described as

$$\begin{aligned} \vec{E}_{in} &= E_{in}\,\hat{p} \\ \vec{E}_x &= E_{in}\hat{p}\cdot\hat{x} = E_{in}\cos\theta_1\cos(\omega t) \\ \vec{E}_y &= E_{in}\hat{p}\cdot\hat{y} = -E_{in}\sin\theta_1\cos(\omega t) \end{aligned} \tag{11}$$

where $\hat{p}$ is a unit vector representing the principle axis of the polaroid, and $\hat{x}$ and $\hat{y}$ are unit vectors corresponding to the axes perpendicular and parallel to the top and bottom surfaces of the waveguide, respectively. We assume that the material in the waveguide has been poled already. That is, it's optical axes are aligned with the x, y, and z axes shown. As these are the principle axes of the material, we can consider the propagation of the x and y polarizations separately in the waveguide.

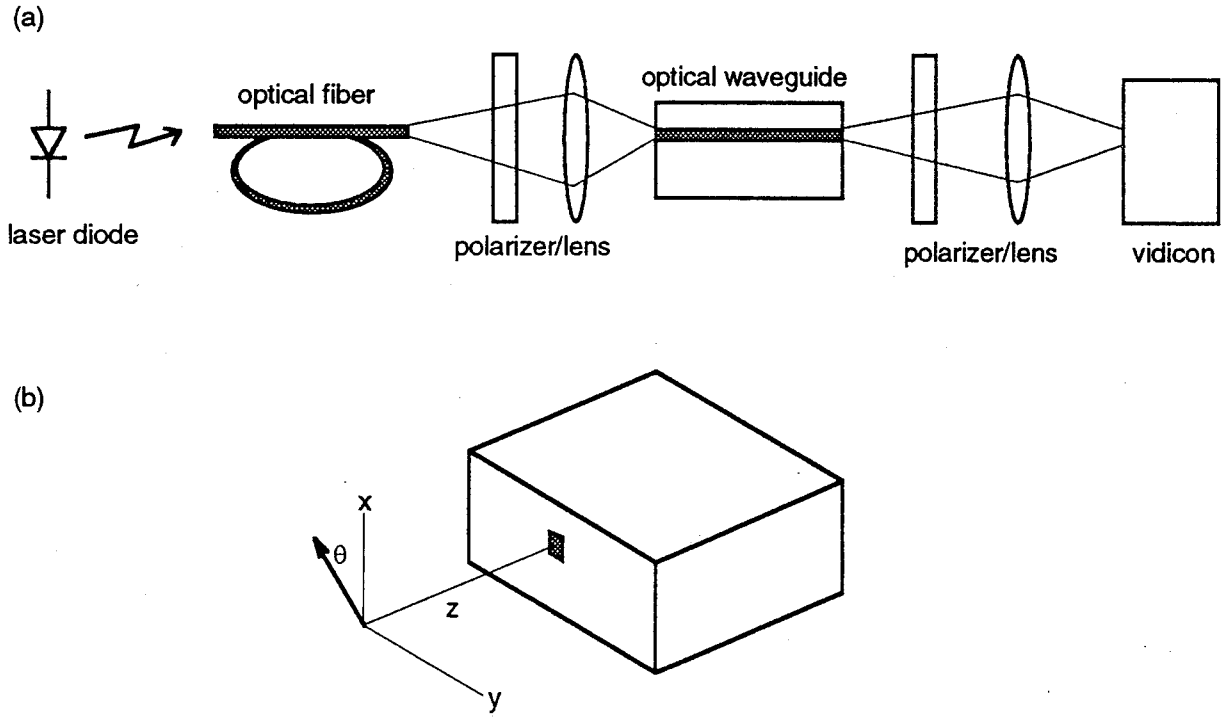

Figure 1. (a) The experimental setup of the transverse modulator used to measure the electrooptic effect. (b) The reference directions for the coordinates axes relative to the optical waveguide. Although shown with a channel waveguide, both channel and slab waveguides can be measured in this system.

The x and y polarizations of the light will propagate through the waveguide independently. Each will experience some phase shift (retardation) and attenuation. In general these will be different for each polarization as the optical properties of the waveguide are different along each of the principle axes.

$$\begin{aligned}\vec{E}_{wg.out} &= E_{x.out}\,\hat{x} + E_{y.out}\,\hat{y} \\ E_{x.out} &= \alpha_x E_{in}\cos\theta_1\cos\left(\omega t + \phi_x\right) \\ E_{y.out} &= -\alpha_y E_{in}\sin\theta_1\cos\left(\omega t + \phi_y\right)\end{aligned} \tag{12}$$

These ϕ's, and possibly α's, will depend on the modulating electric field applied to the waveguide along the x axis, as well as the poling history of the sample.

Now we consider the effect on the output beam. By placing an analyzing polarizer on the output, these two components can be recombined. If the analyzing polarizer is placed at an angle θ_2, then the output light will be

$$\vec{E}_{analyzer.out} = \left[\left(E_{x.out}\,\hat{x} + E_{y.out}\,\hat{y}\right)\cdot\hat{p}_{out}\right]\hat{p}_{out} \tag{13}$$

$$\vec{E}_{analyzer.out} = \left[\alpha_x E_{in}\cos\theta_1\cos\left(\omega t + \phi_x\right)\cos\theta_2 + \alpha_y E_{in}\sin\theta_1\cos\left(\omega t + \phi_y\right)\sin\theta_2\right]\hat{p}_{out}$$

The light intensity will be proportional to the square of the electric field, so the instantaneous intensity is

$$\begin{aligned} I &\propto \vec{E}_{analyzer.out}\cdot\vec{E}_{analyzer.out} \\ &= E_{in}^2\Big(a_x^2\cos^2\left(\omega t + \phi_x\right)\cos^2\theta_1\cos^2\theta_2 \\ &\quad + 2a_x a_y\cos\left(\omega t + \phi_x\right)\cos\left(\omega t + \phi_y\right)\cos\theta_1\cos\theta_2\sin\theta_1\sin\theta_2 \\ &\quad + a_y^2\cos^2\left(\omega t + \phi_y\right)\sin^2\theta_1\sin^2\theta_2\Big)\end{aligned} \tag{14}$$

The intensity averaged over one cycle is

$$\begin{aligned} I \propto \frac{E_{in}^2}{2}\Big(&a_x^2\cos^2\theta_1\cos^2\theta_2 + a_y^2\sin^2\theta_1\sin^2\theta_2 + \frac{2}{T}a_x a_y\cos\theta_1\cos\theta_2\sin\theta_1\sin\theta_2 \\ &\int_0^{T=\frac{2\pi}{\omega}}\cos\left(\omega t + \phi_x\right)\cos\left(\omega t + \phi_y\right)dt\Big)\end{aligned} \tag{15}$$

The integral evaluates to one half $T\cos(\phi_x - \phi_y)$, so the intensity becomes

$$I \propto \frac{E_{in}^2}{2}\left(a_x^2\cos^2\theta_1\cos^2\theta_2 + a_y^2\sin^2\theta_1\sin^2\theta_2 + 2a_xa_y\cos\theta_1\cos\theta_2\sin\theta_1\sin\theta_2\cos\left(\phi_x - \phi_y\right)\right) \quad (16)$$

Now if we assume that the two polarizers are both aligned at 45 degrees, then all the sines and cosines become one over the square root of 2:

$$I \propto \frac{E_{in}^2}{2}\left(\frac{a_x^2}{4} + \frac{a_y^2}{4} + \frac{a_xa_y}{2}\cos\left(\phi_x - \phi_y\right)\right) \quad (17)$$

If now we further assume that the attenuation for the x and y polarizations are equal, then (17) can be simplified to

$$\begin{aligned} I &\propto \frac{E_{in}^2}{4}\left(a^2 + a^2\cos\left(\phi_x - \phi_y\right)\right) \\ &= \frac{a^2E_{in}^2}{4}\left(1 + \cos\left(\phi_x - \phi_y\right)\right) \end{aligned} \quad (18)$$

This shows that the intensity of the light passing through the polarizer is dependant on the relative phase shift between the x and y polarized waves passing through the waveguide. Since the relative phase shift is a function of the applied electric field and the non-linear optical activity of the chromophores added to the waveguide, the intensity will change as the applied electric field is varied.

Finally, to use this technique, we need to understand how to vary the intensity from maximum to minimum. When the difference in the phase of the two polarizations is zero, the cosine is 1 and the intensity is at a peak:

$$I \propto \frac{a^2E_{in}^2}{2} \quad (19)$$

When the phase difference is π, the intensity will be zero. Assuming that the phase difference between the x and y polarizations is proportional to the electric field and hence the applied voltage, the voltage difference required to go from full intensity to zero intensity can be called V_π.

5 Device Fabrication

The fabrication of an electrooptic device based upon organic polymers consists of a large number of processing steps. We have fabricated slab waveguides and single-mode buried waveguides using PMMA and di/tri acrylates. These systems have also been doped with DR-1 and DR-13. The fabrication steps are listed below.

5.1 Material Preparation

DR-13 Solution. Dissolve 3 grams of DR-13 into 20 grams of HPLC grade Acetone. Stir on a hot plate over night.

Cladding Resin. Place the stock container of Ebecryl 4883 Resin in an oven at 50°C to reduce it's viscosity to aid mixing. Mix 47% wt Ebecryl 4883 resin, 50% wt. OTA 480 diluent and 3% wt. Irgacure 184 Photo-initiator in a clean bottle with a magnetic stir rod. Mix in the 50C oven overnight.

Fill a 20cc syringe with the mixed resin and cap the outlet until ready to use.

Core Resin. Place the stock containers of Ebecryl 4883 and Ebecryl 600 Resins in an oven at 50C to reduce their viscosity to aid mixing. Mix 5.9% wt Ebecryl 600 resin, 41.1% wt Ebecryl 4883 resin, 50% wt. OTA 480 diluent and 3% wt. Irgacure 184 Photo-initiator in a clean bottle with a magnetic stir rod. Mix in the 50C oven overnight. This makes the stock core resin. To make the 2% DR-13 doped resin, mix 1.33 grams of the DR-13/Acetone solution per 10.0 grams of the stock core resin in a container that can be tightly sealed. Stir the sealed container on a hot plate set to "Low" (approx. 90C) overnight.

Fill a 20cc syringe with the mixed resin. Attached a cleaned .2 micron filter (Nalgene Cat. No 195-2520) to the syringe and cap the outlet of the filter until ready to use.

Silicon Wafer Preparation. Choose a <100> wafer and cleave to the desired size and shape. Clean both surfaces with Sparkleen detergent and water. Rinse well with DI water. Flood the surface of the wafer with "Buffered HF" hydrofluoric acid solution. Wait for the solution to de-wet from the surface (i.e.. the liquid will pull up into beads). Carefully rinse thoroughly with DI water. Blow dry with filtered GN2 and protect from dust.

3APS Adhesion Promoter. Mix 0.5% wt. 3-aminopropyltriethoxysilane in DI water. Stir well.

5.2 Bottom Cladding

1. Place wafer on spin coater. Center the wafer and adjust speed for 3500 RPM. Set the timer for 45 seconds.

2. Flood surface with 3APS solution and spin (3500RPM for 45 seconds).

3. Using the syringe with cladding resin, press out a circle of resin in the middle of the wafer until the circle is greater than 1/2 the diameter of the wafer. Do this in one squeeze with the outlet of the syringe inside the blob of resin. This prevents entraining air bubbles that result in defects in the film.

4. Reset the spin coater timer to 90 seconds. Spin the cladding layer (3500RPM, 90 seconds)

5. While keeping the sample covered, remove it from the spin coater and place inside the purge box under the UV lamp. Turn on the GN2 purge and purge the box for 6 minutes.

6. Expose to UV light from the Xenon lamp, operated at 1KW, for 2 minutes.

5.3 Core Layer

1. Place the sample on the spin coater. Center the sample and adjust the speed for 2000RPM. Set the timer for 90 seconds. This will produce a film approximately 7 microns thick.

2. Using the syringe with the core resin and filter, press out a circle of resin in the middle of the wafer. This is quite difficult and takes several minutes due to the resistance of the filter. Keep pressing until the circle is about 1/2 the diameter of the wafer.

3. Spin the core resin (2000 RPM, 90 seconds).

4. While the sample is drying on the spin coater, turn on the laser and microscope video monitor. Tune the laser for 6mW, measured at the input to the microscope. Start

LabView and load the PM500 Control VI. Set up for lines written over the desired sample size at 8mm/sec.

5. Using a piece of scrap silicon, set the microscope focus by adjusting the height of the stage, not the microscope focus control! Use the video monitor to verify that the UV spot is in focus. Block the beam to prevent UV from getting to the microscope.

6. Move the sample from the spin coater to the microscope stage, minimizing exposure to dust. Use a drop of water to anchor the wafer to the stage mechanism. With the beam blocked, use the VI "Outline Box" function to verify the correct scan area. When the stage stops, it will be at one corner of the scan area. Remove the beam block and make a final focus adjustment to minimize the size of the bright white UV spot. Replace the beam block.

7. With the beam blocked, start the VI to "Scan Area". The microscope will first move to the center of the sample, and then to one corner. It will then start scanning the first line: remove the beam block now. Adjust the laser power (in "PWR Mode") to get a distinct trail following the spot on the video monitor, but not so much power that side structures are visible. While the lines are being scanned, you can make focus adjustments, but do so only when necessary as it will disturb the lines.

8. When the stage has finished writing the lines, replace the beam block. Before turning off the laser, measure and record the actual beam power.

9. Flush the sample with Acetone quickly until all the red resin is washed off. Quickly blow dry with GN2 while it is still wet with acetone.

The above directions are used to fabricate a channel waveguide. If a slab waveguide is required, follows steps 1-3 and then cure under the UV lamp (step 6, section 5.2). Develop as in step 9 above. The top cladding layer for the slab waveguide is spun on at 3500 RPM for 90 seconds instead of 1500 RPM as described below.

5.4 Top Cladding

1. Place wafer on spin coater. Center the wafer and adjust speed for 1500 RPM. Set the time for 90 seconds.

2. Using the syringe with cladding resin, press out a circle of resin in the middle of the wafer until the circle is greater than 1/2 the diameter of the wafer. Do this in one squeeze with the outlet of the syringe inside the blob of resin. This prevents entraining air bubbles that result in defects in the film.

3. Reset the spin coater timer to 90 seconds. Spin the cladding layer (1500 RPM, 90 seconds). This makes a film about 15 microns thick.

4. While keeping the sample covered, remove it from the spin coater and place inside the purge box under the UV lamp. Turn on the GN2 purge and purge the box for 6 minutes.

5. Expose to UV light from the Xenon lamp, operated at 1KW, for 2 minutes.

5.5 Final Processing

Place the sample in the vacuum bake bell jar and pump a vacuum. Turn on the temperature controller and program for the following cycle and start:

20°C to 100°C ramp over 1 hour

hold at 100°C for 1 hour

100°C to 20°C ramp over 1 hour

20°C hold until stopped.

Figure 2 is a color optical micrograph of the cross-section of a channel waveguide. The core is doped with DR-13. The approximate dimensions of the core region are 9.8 μm tall by 9.1 μm wide. The top and bottom cladding layers are 5 μm thick.

Figure 2. Optical micrograph of the cross-section of a channel waveguide doped with DR-13.

6 Results

In this section, we discuss the fabrication results and measurement results for both slab and channel waveguides.

6.1 Slab waveguide – di/tri acrylate materials – DR-13 chromophore

A slab waveguide is one of the simplest structures to fabricate since no patterning is required. All three layers are fabricated using the UV lamp. The detailed processing steps are covered in Section 5. Figure 3 is an optical micrograph of white light (Fig. 3a) and 1300 nm light (Fig. 3b) guiding in a slab waveguide. This particular sample does not have DR-13 in the core region. The approximate dimensions for this structure are: 10 μm for the lower cladding layer; 9 μm for the core region; and 10 μm for the upper cladding layer. Similar slab waveguides have been fabricated that incorporate the electrooptic molecule, DR-13, into the core region. The sample is then poled and the electrooptic effect is evaluated. A plot of the applied voltage versus the intensity for a DR-13 doped slab waveguide is shown in Figure 4. This data has been fitted to an expected cosinusoid. The value for V_π is obtained from the difference between the x values that produce y_{max} and y=0 in the fitted data. Note that the coefficient on x is in degrees/volt. For this DR-13 slab waveguide, V_π is equal to 865 V. This waveguide was 2.7 cm long so a normalized V_π is 2336 V-cm.

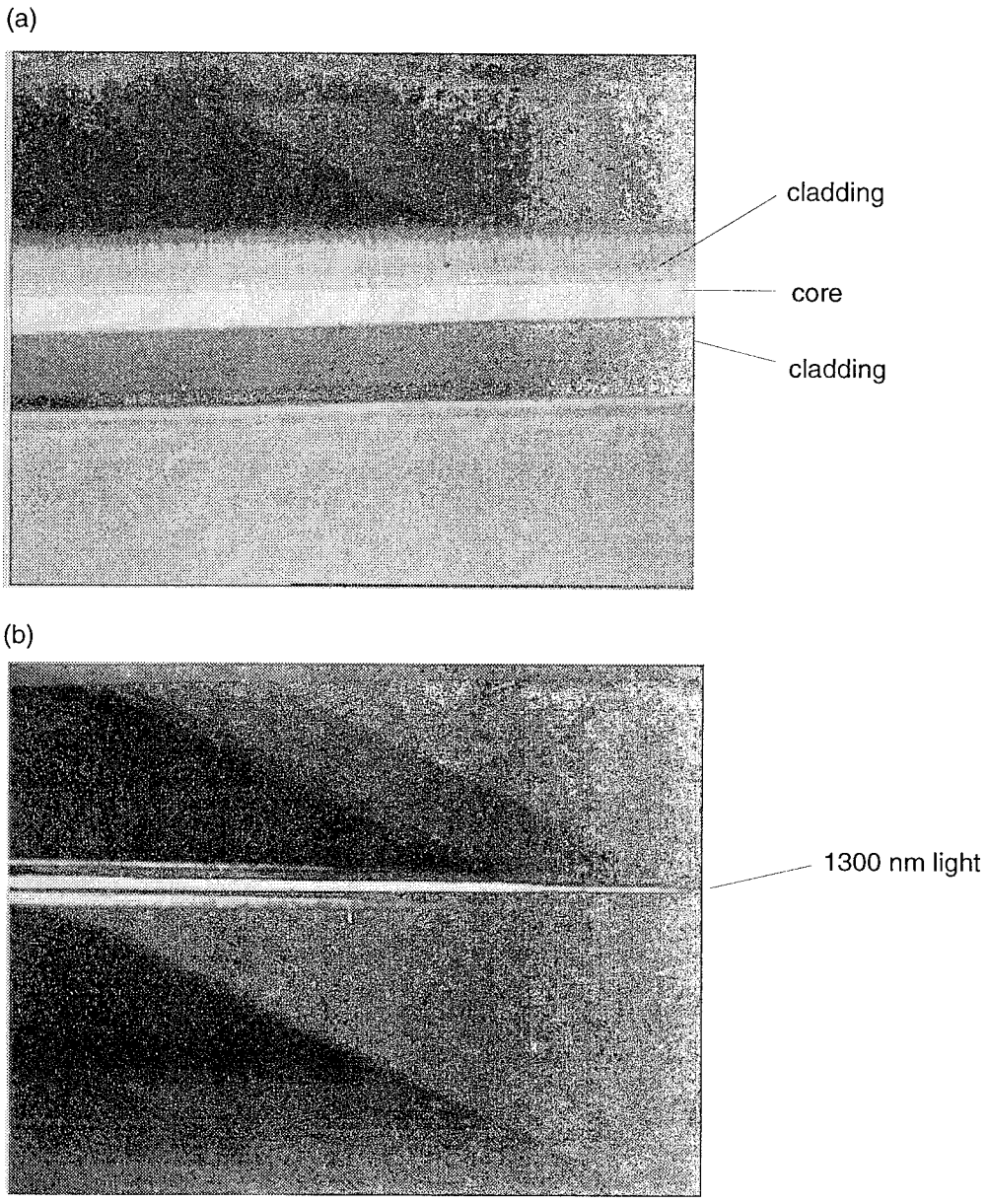

Figure 3. (a) An optical micrograph of a slab waveguide. This image was taken using reflected white light. The core, upper and lower cladding regions are clearly visible. Each layer is approximately 10 μm thick. (b) The same waveguide with 1300 nm light guiding in the core layer.

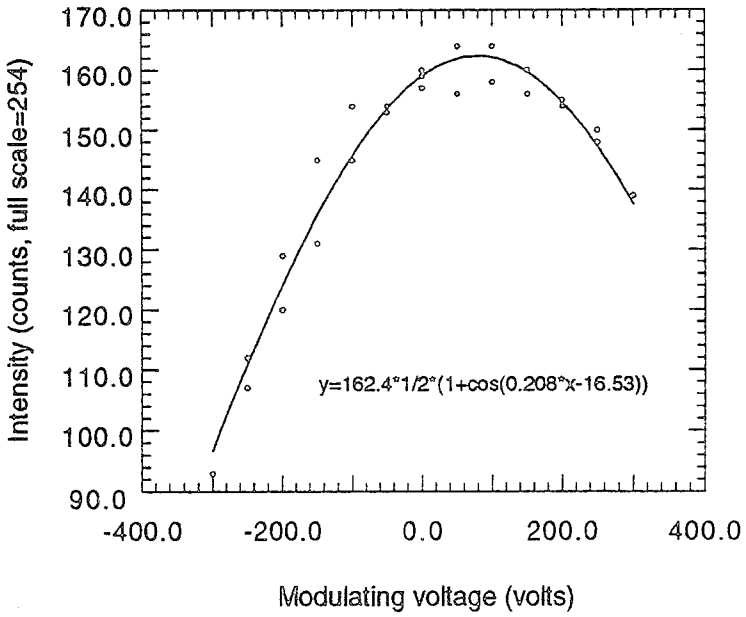

Figure 4. A plot of the intensity versus the applied voltage for a DR-13 doped slab waveguide in the transverse modulator setup. The waveguide was 2.7 cm long. The normalized V_π is equal to 2336 V-cm for this waveguide.

6.2 Slab waveguide – di/tri acrylate materials – DR-1 chromophore

The DR-1 chromophore has been reported on by other investigators [3]. We have studied the same chromophore incorporated into the di/tri acrylate materials. Figure 5 is a plot of the applied voltage versus the intensity for the slab waveguide doped with the DR-1 chromophore. From this data, we can calculate a V_π of 732 V. The waveguide was 4.2 cm long. The normalized V_π is then 3074 V-cm. Comparing this result to that of the DR-13 indicates that the DR-13 system has a normalized V_π of approximately 1.3 times smaller than the DR-1 system. Since V_π is inversely proportional to the electrooptic coefficient, r, this would indicate an increase in r by a factor of 1.3. This confirms our supposition that DR-13 should be a better electrooptic molecule than DR-1. As pointed out previously, we believe this is primarily due to the increased solubility of DR-13 over DR-1.

6.3 Channel waveguide – di/tri acrylate materials – DR-1 & DR-13 chromophores

Although the electrooptic effect is clearly seen in the slab waveguides, device applications require guiding in both dimensions, i.e., a channel waveguide is necessary to ensure high coupling efficiency between other devices in the system. We have constructed single-mode, channel waveguides using the di/tri acrylate system and doped with either DR-1 or DR-13 (See Figure 2. Note the characteristic red color of the DR-13 in the core region.) Unfortunately, to date we have not seen a significant electrooptic effect in the channel waveguides. There could be several reasons for this. First, the core layer in the single-mode channel waveguides is fabricated using the laser writing technique as opposed to the UV lamp in the slab waveguides. This is due to the inability to use contact printing to pattern the single-mode core regions on the tacky acrylate materials. It is plausible that the high photon flux of the laser writing technique may be deactivating the chromophore molecules. Our theoretical analysis of both DR-1 and DR-13 do not support this

hypothesis because the bond energies are generally higher than the 350-360 nm photons of the UV laser. A second possibility is the shape of the waveguide. The channel waveguide may result in significant amounts of the chromophore diffusing into the cladding layers. Figure 2 would tend to dispute this claim however the actual concentration cannot be determined from this micrograph. Several more experiments are underway to determine the discrepancy between the electrooptic effect in slab versus channel waveguides.

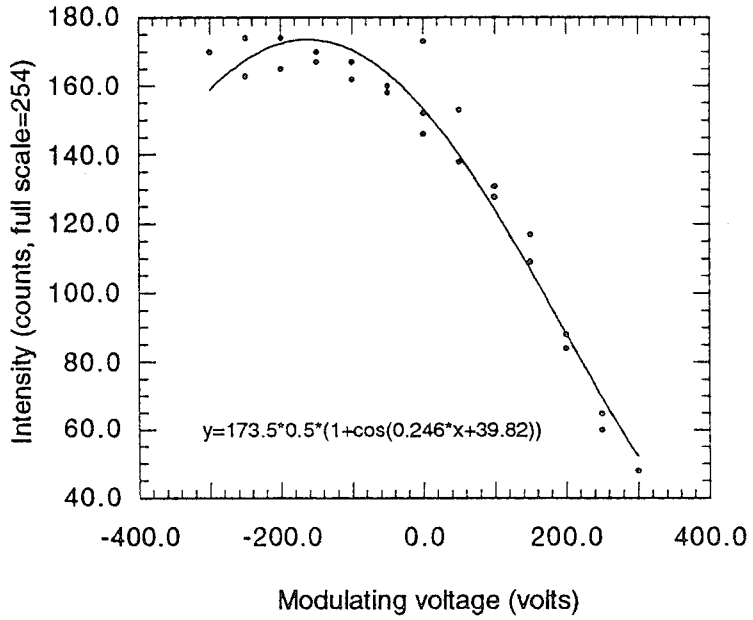

Figure 5. A plot of the intensity versus the applied voltage for a DR-1 doped slab waveguide in the transverse modulator setup. The waveguide was 4.2 cm long. The normalized V_π is equal to 3074 V-cm for this waveguide.

7 Summary

Several important preliminary conclusions can be drawn from the work to date. The importance of the concentration of the chromophore is evidenced by the normalized (equal interaction length) V_π obtained for the DR-1 and DR-13 slab waveguides. The normalized V_π for DR-13 is 2336 V-cm while the normalized V_π for DR-1 is 3074 V-cm. The solubility of DR-13 in acetone is approximately 3 times that of DR-1 and is believed to be responsible for the lower V_π in the DR-13 samples. However, the V_π values obtained are quite low. This indicates that the electrooptic coefficient is quite low (detailed calculations are underway).

Upon exploring the channel waveguide, we see a further reduction in the normalized V_π. At the present time, we do not understand this further reduction in V_π for a channel waveguide compared to a slab waveguide.

There are several possible explanations for these low electrooptic effects. Ultraviolet light used in the photopolymerization process may be responsible for breaking bonds in the chromophore and thus rendering it inactive. The photoexcited free radicals (obtained from the photodissociation of the initiator molecules) may also be reacting with the chromophore and producing an inactive chromophore. Finally, the solvent rinses use during device fabrication may be leaching out the

chromophore and significantly reducing the chromophore concentration. These effects are currently being investigated.

While the final explanation of the reduced V_π values is still under investigation, it is apparent that processing these materials into working devices, e.g., channel waveguides versus slab waveguides, can have a detrimental effect on the electrooptic coefficient. While material characterization that specifically measures the molecular electrooptic coefficient of the chromophore is important, it must be corroborated with characterization techniques that measure the effect of material processing on the chromophore's electrooptic effect.

8 References

[1] S. R. Marder, "Optimization of Microscopic and Macroscopic Second-Order Optical Nonlinearities," in *Materials Chemistry – An Emerging Discipline*, L. V. Interrante, L. A. Caspar, and A. B. Ellis, Eds., Washington, DC: American Chemical Society, 1995, pp. 189-210.

[2] K. Nakagawa, T. Kowalewski, C.W. Phelps, D.L. Rode and R.R. Krchnavek, "Optical Channel Waveguides Based On Photo-Polymerizable Di/Tri Acrylates," in *Optoelectronic Interconnects II*, Ray T. Chen, John A. Neff, Editors, Proc. SPIE 2153, 1994, pp. 208-217.

[3] R. H. Page, M, C. Jurich, B. Reck, A. Sen, R. J. Twieg, J. D. Swalen, G. C. Bjorklund and C. G. Willson, "Electrochromic and optical waveguide studies of corona-poled electro-optic polymer films," in *J. Opt. Soc. Am.,* B, vol. 7, No. 7, July 1990.

*U.S. GOVERNMENT PRINTING OFFICE: 1996-710-126-20158

MISSION

OF

ROME LABORATORY

Mission. The mission of Rome Laboratory is to advance the science and technologies of command, control, communications and intelligence and to transition them into systems to meet customer needs. To achieve this, Rome Lab:

a. Conducts vigorous research, development and test programs in all applicable technologies;

b. Transitions technology to current and future systems to improve operational capability, readiness, and supportability;

c. Provides a full range of technical support to Air Force Materiel Command product centers and other Air Force organizations;

d. Promotes transfer of technology to the private sector;

e. Maintains leading edge technological expertise in the areas of surveillance, communications, command and control, intelligence, reliability science, electro-magnetic technology, photonics, signal processing, and computational science.

The thrust areas of technical competence include: Surveillance, Communications, Command and Control, Intelligence, Signal Processing, Computer Science and Technology, Electromagnetic Technology, Photonics and Reliability Sciences.